Spontaneous Insertion, Helix Formation, and Hydration of Polyethylene Oxide in Carbon Nanotubes

Udaya R. Dahal and Elena E. Dormidontova*
Polymer Program, Institute of Materials Science and Physics Department, University of Connecticut, Storrs, Connecticut 06269, USA
(Received 30 March 2016; published 6 July 2016)

Hydration strongly affects macromolecular conformation in solution and under nanoconfinement as encountered in nature and nanomaterials. Using atomistic molecular dynamics simulations we demonstrate that polyethylene oxide spontaneously enters single wall carbon nanotubes (CNTs) from aqueous solutions and forms rodlike, helix, and wrapped chain conformations depending on the CNT diameter. We show that water organization and the stability of the polyethylene oxide hydration shell under confinement is responsible for the helix formation, which can have significant implications for nanomaterial design.

DOI: 10.1103/PhysRevLett.117.027801

Introduction.—With the rapid development of nanotechnology the exposure of macromolecules to nanoconfinement has become more common. Many material properties, such as biodegradability, ionization, and charge transport are affected by water mobility and accessibility to the polymer under confinement. A better understanding of interactions and conformational changes for macromolecules under nanoconfinement is required to improve nanomaterial design and anticipate the effect of nanomaterials on the environment. The effect of confinement on the behavior of biopolymers has been actively discussed, as nanopores and nanoconfinement are commonly encountered in biology [1–12]. However, a complete understanding has not been achieved so far due to both the complexity of the systems and variations in the outcome of nanoconfinement of biopolymers; e.g., in some cases a helical structure is stabilized and in others it is destabilized [3,4,6,13]. Biopolymer hydration is recognized as an important factor affecting their secondary and ternary structure with a few reports discussing hydration effects under confinement [6,14]. In contrast to biopolymers, synthetic polymers, which are commonly used in nanomaterial design, do not exhibit a secondary structure, but some can form hydrogen bonds with water which ensures their solubility [15–17]. The effect of hydration on polymer conformation under confinement has not been considered so far, as theoretical discussion was focused on conformational limitations imposed on polymer-biopolymer by confinement [11,18,19] with only a few computer modeling reports of nonpolar polymers entering carbon nanotubes (CNTs) from solution [20,21]. Since the structure and properties (e.g., diffusion) of water under confinement, e.g., inside CNTs, is quite different from bulk solution [22–26], it is logical to expect that hydration of water-soluble polymers will be different under confinement. Polyethylene oxide (PEO), which is considered in this Letter, is a water-soluble polymer actively used in biomedical applications due to its biocompatibility and propensity to inhibit protein adsorption [27,28]. Understanding PEO behavior under nanoconfinement can also be important for developing PEO-based nanocomposites, separation or sensing membranes, and energy applications [29,30]. Elucidation of the water arrangement around the polymer is challenging experimentally due to the required subnanoscale resolution. Atomistic molecular dynamics simulations can provide the necessary level of molecular detail to address this issue and make experimentally testable predictions, therefore stimulating and guiding future experimental research.

In this Letter, using atomistic molecular dynamics simulations we study the spontaneous insertion of a PEO chain into CNTs from aqueous solution and investigate the equilibrium polymer conformation inside the CNTs as a function of nanotube diameter. We elucidate the key role that water plays in this phenomenon and analyze the water arrangement around the confined polymer to explain the physical origin of the unusual PEO helix formation and its stability inside the CNT. We also make experimentally testable predictions regarding the conditions under which water-soluble polymers can be spontaneously encapsulated into nanochannels and demonstrate the importance of hydration under nanoconfinement for polymer properties that are essential for nanomaterial design and applications.

Model.—All MD simulations were performed using the GPU version of GROMACS 4.6.5. [31] with OPLS all atom force field [32]. Unless otherwise specified the methyl-terminated polyethylene oxide contained 36 repeat units. In all simulations CNTs were of finite length (typically 15 nm) oriented in the z direction, neutral, and fixed (frozen). The specifics of the model and simulation protocol are described in the Supplemental Material [33]. Periodic boundary conditions were implemented in all dimensions with the box size (typically 4 nm × 4 nm × 25 nm) chosen to accommodate the CNTs and polymer, surrounded by SPC/E (simple point charge extended model) water from all

sides. All simulations were performed at $T = 288$ K using the Berendsen thermostat. To calculate hydrogen bonding between PEO and water we used geometric criteria: $r \leq 3.5$ Å for the distance between donor and acceptor groups and $\theta \leq 30°$ for the hydrogen-donor-acceptor angle. All visualizations were done using VMD (visual molecular dynamics) [34].

Results.—To study the interactions between the CNT and PEO in aqueous solution the chain was placed and equilibrated in the vicinity, but outside the nanotube. When a polymer chain finds itself in the vicinity of the outer surface of the CNT a weak polymer adsorption without wrapping around the CNT is observed, in agreement with results of previous MD simulations [43]. When one of the ends of the PEO chain finds its way into a nanotube a spontaneous and rapid insertion of PEO into the nanotube occurs [44]. Figure 1 shows the change in PEO coordinates upon insertion into a 8-8 CNT of 1.085 nm diameter $(d = (n^2 + m^2 + nm)^{1/2} \times 0.0783$ nm with $n = 8$ and $m = 8$ being the chiral indices). After about 1 ns from the beginning of the process a portion of the chain containing 8 repeat units (out of a total 36) have entered into the CNT and assumed a helical conformation [Fig. 1(b)]. After another 1 ns the majority of the chain (24 repeat units) was inside the CNT in a helical conformation [Fig. 1(c)]. The whole process of PEO encapsulation into the CNT took about 3.5 ns. Additional simulation runs showed qualitatively and quantitatively similar results with the characteristic encapsulation time being approximately the same: 3.5 ns $\pm$ 0.5 ns. The same phenomenon of spontaneous chain insertion was observed for PEO of different lengths (e.g., a PEO chain of 18 repeat units took 1.4 ns $\pm$ 0.5 ns to enter the same CNT) and for CNTs of different diameters.

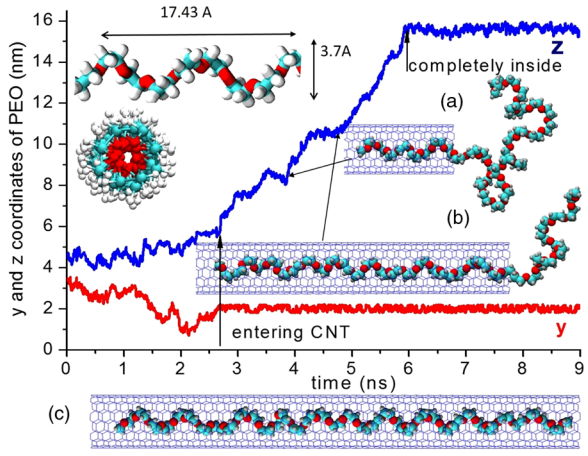

FIG. 1. The coordinates (y, perpendicular and z, along the CNT) of the PEO center of mass ($N = 36$) as a function of time and simulation snapshots showing the chain conformation at (a) 1, (b) 2, and (c) 3.5 ns after entering the CNT with a zoom-in view of the helix period and a rear view (inset). In all snapshots water is removed for clarity, oxygen and carbon atoms are shown as red and cyan balls, respectively, hydrogen as small gray or white balls.

Insertion of PEO ($N = 36$) into the narrow tubes (0.95 nm $\leq d \leq$ 1.15 nm) occurs more rapidly (i.e., with a larger velocity) once the process started than that for wider tubes [33]. This result may seem surprising taking into account that entering a narrow tube requires a more dramatic change of polymer conformation. However, the dynamics of water in narrow tubes is known to be very facile due to single file diffusion [22–24] and, as will be discussed below, water substitution by PEO is one of the important factors in the process.

After the complete encapsulation the PEO chain remains in a helical conformation inside the 8-8 CNT without exiting the tube. We characterized the properties of the helix and arrived at a diameter of 3.7 Å (from carbon to carbon) with about 7 repeat units per period of 17.43 Å (Fig. 1) leading to 2.49 Å for the helix rise (i.e., the pitch per repeat unit), which corresponds to the so-called 3_{10} helix in Bragg's nomenclature. The properties of the helix are close to that for the PEO helix formed in the crystal state, a 7/2 helix with 7 repeat units per 19.48 Å helix period and a diameter of 3.3–3.5 Å [45–48], except the PEO helix inside the 8-8 CNT containing water is somewhat shorter and wider. The difference is most likely attributed to the water associated with a helix inside the CNT, as in a more narrow CNT (4-11) with less water the helix structure (period 18.2 Å, diameter 3.5 Å) is closer to that in a crystal state, while in CNTs of larger diameters (1.2–1.3 nm for 9-9, 9-10) containing more water, the PEO helix becomes even shorter (period 15.4–15.8 Å) and wider (4.8–5.4 Å) with 9-10 repeat units per period.

To investigate the PEO conformation under nanoconfinement we studied a range of CNTs of different diameters d from 0.95 (7-7) to 2.7 nm (20-20) into which the PEO chain spontaneously infiltrates [33]. To characterize the chain conformation we analyzed the average end-to-end distance R_{end}, radius of gyration R_g, and their ratio R_{end}/R_g, which are shown (except for R_g) as a function of CNT diameter in Fig. 2. As is seen, in the most narrow CNTs (7-7, 7-8) PEO is strongly stretched (e.g., $R_{\text{end}} = 12.8$ nm in CNT 7-7 is nearly 3 times larger than the solution value of $R_{\text{end solution}} = 4.1$ nm) forming a rodlike conformation, with R_{end}/R_g approaching $\sqrt{12}$. Obviously, such chain stretching is highly unfavorable entropically, leading to an estimated conformational free energy loss of about 13 kT, [based on the simple Flory-like expression $3kTR^2_{\text{end}}/(2R^2_{\text{end solution}})$ [49], where k is the Boltzmann constant], not to mention the loss in the energy of hydrogen bonding between PEO and water (1.2 hydrogen bonds with energy about 19 kJ/mol per oxygen in solution vs no hydrogen bonds in CNT 7-7). For this conformation to be thermodynamically stable there has to be some strong counterbalancing benefit for the system, which can be the liberation of water that gains 0.8 hydrogen bonds (i.e., about 11.4 kJ/mol) per molecule moving from CNT to solution [33]. As a PEO chain of 36 repeat units replaces approximately 65 water molecules inside the nanotube

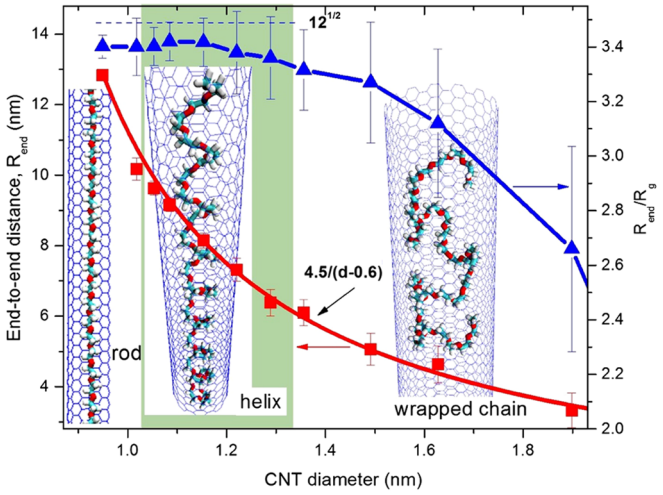

FIG. 2. The average end-to-end distance R_{end} (squares) fitted by Eq. (1) (with $R_{\mathrm{end\,solution}} = 4.1$ nm) and the ratio R_{end}/R_g (triangles) for the PEO chain inside the CNT as functions of the CNT diameter. The horizontal dashed line indicates $R_{\mathrm{end}}/R_g = \sqrt{12}$, the expected value for a rigid rod. Snapshots of the PEO chain inside the CNT representing three conformational regimes: rod, helix, and chain wrapped along the inner CNT surface (representation similar to Fig. 1).

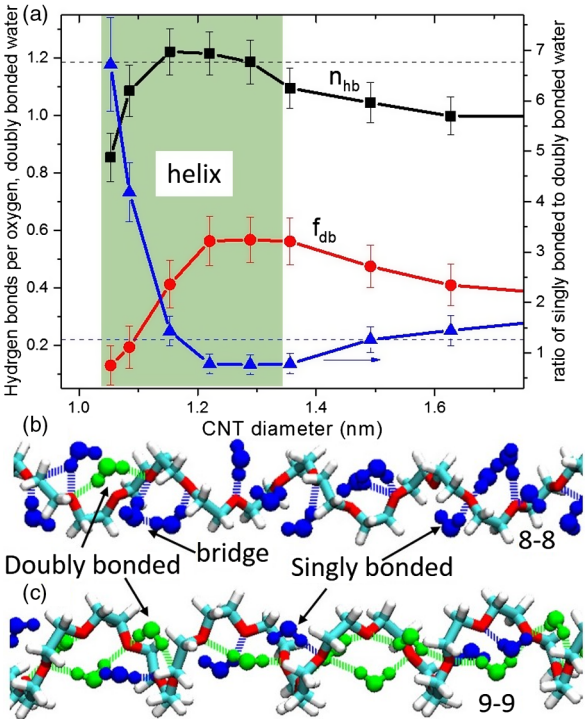

FIG. 3. (a) The average number of hydrogen bonds per oxygen of PEO, n_{hb} (squares), the fraction of water doubly bound to PEO, f_{db} (circles), and the ratio of singly to doubly bonded water (triangles) vs the CNT diameter. The horizontal dashed lines mark n_{hb} and the ratio of singly to doubly bonded water for aqueous solutions of PEO. Simulation snapshots (same representation as in Fig. 1) of sections of the PEO helix with singly bonded (blue) and doubly bonded (green) water molecules together with the corresponding hydrogen bonds for 8-8 (b) and 9-9 (c) CNTs.

(nearly independently of the CNT diameter) the free energy change due to the water gain and PEO loss in hydrogen bonding is about −55.8 kJ/mol or −23.3 kT (at $T = 288$ K), as shown in the Supplemental Material [33]. This exceeds the loss in conformational entropy of the chain at least for narrow CNTs (7-7, 7-8), and can explain the observed spontaneous chain insertion. We note that PEO-CNT [43], water-CNT interactions and translational entropy of water [50,51], also contribute to the chain insertion free energy, making its calculation rather challenging and requiring further detailed investigation.

In CNTs of larger diameter ($d = 1.05$–1.3 nm) water forms a shell well interconnected by hydrogen bonding at a level approaching the bulk solution value [23,24]. In these CNTs PEO forms a helix with R_{end}/R_g remaining close to the rigid rod value of $\sqrt{12}$ despite the intrinsic flexibility of PEO (persistence length 3.7 Å) [52]. As the CNT diameter increases the helix becomes noticeably shorter and wider to accommodate the increasing number of water molecules participating in PEO hydration and R_{end} starts to decline. The decrease of R_{end} with CNT diameter does not follow any classical models [11,18,19], but can be well described [somewhat in the spirit of Eq. (10) of Ref. [53]] by

$$\frac{R_{\mathrm{end}}}{R_{\mathrm{end\,solution}}} = \frac{1.1}{d_{\mathrm{eff}}} = \frac{1.1}{(d-0.6)}, \qquad (1)$$

with $d_{\mathrm{eff}} = 2r_{\mathrm{efff}} = d - 0.6$ nm being the polymer-accessible radius of the tube. r_{eff} corresponds to the CNT radius reduced by an exclusion zone width, 0.3 nm, which is the average separation of the PEO hydrogens from the CNT inner surface [33]. The implication of Eq. (1), which remains valid over the whole studied d range, is that the effective surface area of PEO-CNT contact, $2\pi r_{\mathrm{eff}} R_{\mathrm{end}}$, remains constant with an increase of CNT diameter.

To understand the origin of helix formation we characterized PEO hydration inside the CNT by calculating the average number of hydrogen bonds per oxygen of PEO, n_{hb}, which is shown in Fig. 3. As is seen, for 4-11 ($d = 1.053$ nm) and 8-8 CNTs ($d = 1.085$ nm), n_{hb} and, correspondingly, the number of water molecules hydrogen bonded to PEO, $N_w{}^{\mathrm{hb}}$, is noticeably smaller than in aqueous solution, while in 8-9, 9-9, and 9-10 CNTs ($d = 1.153$–1.29 nm), n_{hb} and N_w are close to the solution values. To gain further insights into water arrangements around the PEO helix, we categorized water hydrogen bonded to PEO into two classes: "singly bonded water" forming a single bond with PEO and "doubly bonded water" having two hydrogen bonds with two different oxygens of PEO, usually the i and $i+2$ oxygens of PEO, as is seen in Fig. 3(c). The doubly bound water is of particular interest in understanding the physical origin of helix stabilization inside the CNT, as it brings together a section of the PEO chain in the TGT conformation, which favors helix formation. In 9-9 and 9-10 CNTs the fraction

of doubly bound water (relative to the total number N_w), n_{db} exceeds that for aqueous solution, resulting in an average of 4 double-bonded waters per helix period [Fig. 3(c)]. These doubly bound waters play a role analogous to the intramolecular hydrogen bonding in biopolymers that are responsible for their helical structure. In 8-9 CNT ($d = 1.153$ nm) there are on average 3 doubly bonded waters per helix period with n_{db} comparable to bulk solution where PEO does not form a helix. In the narrow 4-11 and 8-8 CNTs, there is insufficient space to form multiple bridges between the i and $i + 2$ oxygens by doubly bonded water, so singly bonded water dominates, as is seen in Figs. 3(a), 3(b). While there are some hydrogen bonded bridges between singly bonded waters, as is seen in Fig. 3(b), which can help to hold together the helix structure, there must be some additional factors that play a role in helix structure stabilization.

One possible reason for helix stabilization is a higher stability of the PEO hydration shell inside the CNT compared to solution. To quantify this effect we selected water hydrogens bonded to PEO inside the CNT at $t = 0$, $N_w(0)$ and calculated the following correlation function $C(t)$:

$$C(t) = \left\langle \frac{N_w(t)}{N_w(0)} \right\rangle, \tag{2}$$

where $N_w(t)$ is the number of water molecules among the initially selected ones that remain hydrogen bonded (but not necessarily to the same PEO oxygen) at time t and $\langle \ldots \rangle$ denotes averaging over different initial states. Thus, the larger $C(t)$ is, the larger is the fraction of long-lasting waters in the hydration shell of PEO, even though this water may not be continuously bound to PEO. As is seen from Fig. 4, for a given CNT diameter $C(t)$ first abruptly decreases and then stabilizes at some plateaulike level. In the narrow CNTs (4-11, 8-8, 8-9) more than 70% of the water remains in the PEO hydration shell for more than 1 ns (for comparison the characteristic lifetime of a PEO-water hydrogen bond is about 4–5 ps [54]). This result is not that surprising, as water diffusion inside the corresponding CNTs is known to be rather limited, based on the results of MD simulations [23–25]. The presence of PEO is likely to further slow down the water diffusion inside the CNT. Thus, the stability of the PEO hydration shell is likely to be the main factor in helix stabilization inside the CNTs, as near the chain ends where water moves more freely the helical conformation is noticeably less stable compared to the middle of the chain [33]. Since the contribution of chain ends is larger for shorter chains, one should expect that short PEO chains are less likely to form a stable helix, as is indeed the case [33]. For CNTs of somewhat larger diameter, such as 9-9 and 9-10 ($d = 1.22$ nm and $d = 1.29$ nm) the fraction of long-lasting water in the hydration shell decreases to 40%–50%, but recall that the fraction of doubly bonded water acting as intramolecular cross-links for the helix is larger in this case, so the helical

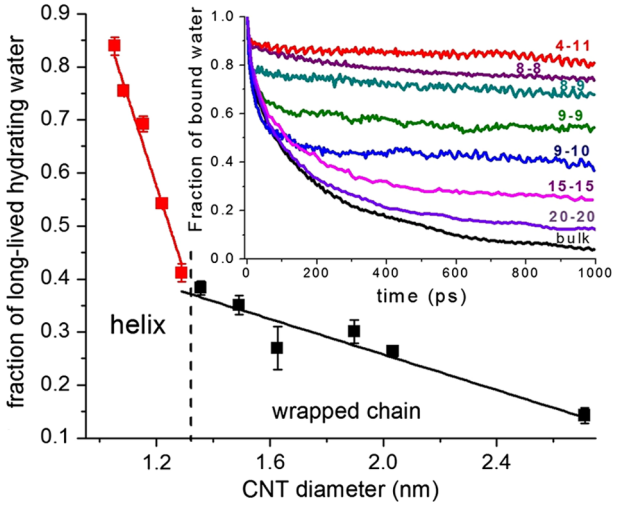

FIG. 4. The average fraction of long-lasting water in a PEO hydration shell corresponding to the plateau value of the correlation function $C(t)$ [Eq. (2)] (shown in the inset as a function of time for different CNTs), as a function of CNT diameter. The best linear fits to the data for helices and wrapped chains, respectively, are shown as solid lines. The vertical dashed line indicates the boundary between helix and wrapped chain regimes.

structure remains stable. Since the decay in $C(t)$ is associated with the exchange of water hydrogen bonded to PEO and free water in its vicinity, the plateau value of the fraction of long-lasting water in the hydration shell should linearly decrease with the amount of free water, which in turn scales with CNT diameter, as indeed is seen in Fig. 4, where the plateau value of $C(t)$ is plotted as a function of CNT diameter.

In CNTs with a diameter exceeding 1.3 nm the number of free waters exceeds those hydrogens bonded to PEO, so the waters initially in the hydration shell of PEO can now diffuse away from the polymer almost as easily as in solution. Accordingly, the correlation function $C(t)$ exhibits a somewhat different pattern with a more continuous decay and a smaller fraction of long-lasting waters in the hydration shell (Fig. 4), which is insufficient to support the helix structure and, consequently, the PEO chain wraps along the inner surface of the CNT, as is seen in Fig. 2. The fraction of long-lasting water in the hydration shell of wrapped PEO systematically decreases following a somewhat different linear dependence on the CNT diameter than for the PEO helices (Fig. 4), since now the most stable water is that in the layer interfacing with the CNT with the degree of hydrogen bonding between PEO and water being somewhat smaller than in aqueous solution. The observed change in slopes seen in Fig. 4 is indicative of different water dynamics inside the CNT and delineates the transition from helix to wrapped chain regimes. For the wider CNTs the dominant factor for water replacement by PEO becomes the minimization of less favorable water-CNT contacts. In the limit of wide CNTs we expect that any

preference for the PEO chain wrapping the inner compared to the outer CNT surface will vanish.

In summary, based on the results of our atomistic molecular dynamics simulations we show that a polyethylene oxide chain spontaneously enters carbon nanotubes of different sizes from aqueous solution. Rapid chain insertion occurs for narrow CNTs ($0.95\ \text{nm} \leq d \leq 1.15\ \text{nm}$) with highly mobile structured water inside and slows down with increasing tube diameter. Inside CNTs PEO forms a rodlike, helical, or wrapped (along the inner CNT surface) chain conformation depending on the CNT diameter (Fig. 2). We show that the high stability of the PEO hydration shell inside the CNT is a key factor in helix formation (Fig. 4), with doubly bound water playing the role of intramolecular cross-links (Fig. 3). These results provide molecular level insights into the role of water in PEO helix formation and imply that relatively immobile water (or other hydrogen bond-donating solvents) is necessary for helix formation. The obtained results also suggest a new method of PEO (or other amphiphilic water-soluble polymer) encapsulation in nanopores and demonstrate the importance of understanding hydration for predicting the behavior of macromolecules under nanoconfinement, which can be further explored in future experimental and theoretical research, and used in designing nanomaterials for biomedical, sensing and energy applications.

This work was supported by the National Science Foundation Grant No. DMR-1410928. Data analysis was partially conducted at the High Performance Computing Cluster at the University of Connecticut.

*Corresponding author.
elena@uconn.edu

[1] K. A. Dill, S. Bromberg, K. Yue, K. M. Fiebig, D. P. Yee, P. D. Thomas, and H. S. Chan, Protein Sci. **4**, 561 (1995).
[2] T. Tian and A. E. Garcia, J. Am. Chem. Soc. **133**, 15157 (2011).
[3] E. P. O'Brien, G. Stan, D. Thirumalai, and B. R. Brooks, Nano Lett. **8**, 3702 (2008).
[4] G. Ziv, G. Haran, and D. Thirumalai, Proc. Natl. Acad. Sci. U.S.A. **102**, 18956 (2005).
[5] J. Gumbart, C. Chipot, and K. Schulten, J. Am. Chem. Soc. **133**, 7602 (2011).
[6] M. B. Ulmschneider, J. K. Leman, H. Fennell, and O. Beckstein, J. Membr. Biol. **248**, 407 (2015).
[7] S. H. White and G. von Heijne, Annu. Rev. Biophys. **37**, 23 (2008).
[8] S. H. White, FEBS Lett. **555**, 116 (2003).
[9] M. Muthukumar and C. Y. Kong, Proc. Natl. Acad. Sci. U.S.A. **103**, 5273 (2006).
[10] M. Muthukumar, Annu. Rev. Biophys. Biomol. Struct. **36**, 435 (2007).
[11] W. Reisner, J. N. Pedersen, and R. H. Austin, Rep. Prog. Phys. **75**, 106601 (2012).
[12] W. Reisner, K. J. Morton, R. Riehn, Y. M. Wang, Z. Yu, M. Rosen, J. C. Sturm, S. Y. Chou, E. Frey, and R. H. Austin, Phys. Rev. Lett. **94**, 196101 (2005).
[13] H-X. Zhou, J. Chem. Phys. **127**, 245101 (2007).
[14] Y. Xue and M. Chen, Nanotechnology **17**, 5216 (2006).
[15] E. E. Dormidontova, Macromolecules **35**, 987 (2002).
[16] E. E. Dormidontova, Macromolecules **37**, 7747 (2004).
[17] P. Molyneux, *Water-Soluble Synthetic Polymers: Properties and Behavior* (CRC Press, Boca Raton, 1983).
[18] T. Odijk, Macromolecules **16**, 1340 (1983).
[19] P. G. de Gennes, *Scaling Concepts in Polymer Physics* (Cornell University Press, Ithaca, NY, 1979).
[20] C. Wei and D. Srivastava, Phys. Rev. Lett. **91**, 235901 (2003).
[21] P. P. Wanjari, A. V. Sangwai, and H. S. Ashbaugh, Phys. Chem. Chem. Phys. **14**, 2702 (2012).
[22] A. Alexiadis and S. Kassinos, Chem. Rev. **108**, 5014 (2008).
[23] R. J. Mashl, S. Joseph, N. R. Aluru, and E. Jakobsson, Nano Lett. **3**, 589 (2003).
[24] H. Ye, H. Zhang, Y. Zheng, and Z. Zhang, Microfluid Nanofluid **10**, 1359 (2011).
[25] A. I. Kolesnikov, J-M. Zanotti, C-K. Loong, P. Thiyagarajan, A. P. Moravsky, R. O. Loutfy, and C. J. Burnham, Phys. Rev. Lett. **93**, 035503 (2004).
[26] A. Striolo, Nano Lett. **6**, 633 (2006).
[27] J. M. Harris, *Introduction to Biotechnical and Biomedical Applications of Poly(Ethylene Glycol)*, Topics in Applied Chemistry (Springer, New York, 1992), p. 1–14.
[28] J. H. Lee, H. B. Lee, and J. D. Andrade, Prog. Polym. Sci. **20**, 1043 (1995).
[29] Q. Zhang and L. A. Archer, Langmuir **18**, 10435 (2002).
[30] I. Honma, S. Nomura, and H. Nakajima, J. Membr. Sci. **185**, 83 (2001).
[31] M. J. Abraham, T. Murtola, R. Schulz, S. Páll, J. C. Smith, B. Hess, and E. Lindahl, SoftwareX **1–2**, 19 (2015).
[32] W. L. Jorgensen, D. S. Maxwell, and J. Tirado-Rives, J. Am. Chem. Soc. **118**, 11225 (1996).
[33] See Supplemental Material at http://link.aps.org/supplemental/10.1103/PhysRevLett.117.027801 for simulation details; velocity of PEO insertion into CNT; estimation of hydrogen bonding energy change upon insertion; average distance between hydrogens of PEO and CNT; correlation functions for the fraction of long-lasting water for the middle and chain ends, as well as for shorter chain ($N = 9$); simulation snapshots for short PEO ($N = 9$) inside 9-9 CNT, which contains Refs. [34–42].
[34] W. Humphrey, A. Dalke, and K. Schulten, J. Mol. Graphics **14**, 33 (1996).
[35] S. Hezaveh, S. Samanta, G. Milano, and D. Roccatano, J. Chem. Phys. **135**, 164501 (2011).
[36] B. Z. Shang, Z. Wang, and R. G. Larson, J. Phys. Chem. B **112**, 2888 (2008).
[37] D. van der Spoel, P. J. van Maaren, P. Larsson, and N. Timneanu, J. Phys. Chem. B **110**, 4393 (2006).
[38] F. Franks, *Water a Comprehensive Treatise* (Plenum, New York, 1973).
[39] W. A. P. Luck, Discuss. Faraday Soc. **43**, 115 (1967).
[40] G. Scatchard, G. M. Kavanagh, and L. B. Ticknor, J. Am. Chem. Soc. **74**, 3715 (1952).
[41] G. E. Walrafen, J. Chem. Phys. **40**, 3249 (1964); **44**, 1546 (1966).

[42] S. Lusse and K. Arnold, Macromolecules **29**, 4251 (1996).
[43] S. Rouhi, Y. Alizadeh, and R. Ansari, Braz. J. Phys. **45**, 10 (2015).
[44] See Supplemental Material at http://link.aps.org/supplemental/10.1103/PhysRevLett.117.027801 for the movie showing PEO chain ($N = 36$) insertion into a CNT 8-8 nanotube with all the water inside and a fraction of the water outside the nanotube along the cylindrical axis shown.
[45] Y. Takahashi and H. Tadokoro, Macromolecules **6**, 672 (1973).
[46] K. Maranski, Y. G. Andreev, and P. G. Bruce, Angew. Chem. Int. Ed. **53**, 6411 (2014).
[47] D. Seebach, E. Zass, W. B. Schweizer, A. J. Thompson, A. French, B. G. Davis, G. Kyd, and I. J. Bruno, Angew. Chem. Int. Ed. **48**, 9596 (2009).
[48] A. C. French, A. L. Thompson, and B. G. Davis, Angew. Chem. Int. Ed. **48**, 1248 (2009).
[49] M. Rubinstein and R. H. Colby, *Polymer Physics* (Oxford University Press, Oxford, 2003).
[50] G. Perez-Hernandez and B. Schmidt, Phys. Chem. Chem. Phys. **15**, 4995 (2013).
[51] T. A. Pascala, W. A. Goddarda, and Y. Junga, Proc. Natl. Acad. Sci. U.S.A. **108**, 11794 (2011).
[52] H. Lee, R. M. Venable, A. D. MacKerell, Jr., and R. W. Pastor, Biophys. J. **95**, 1590 (2008).
[53] D. R. Tree, Y. Wang, and K. D. Dorfman, Phys. Rev. Lett. **110**, 208103 (2013).
[54] O. Borodin, D. Bedrov, and G. D. Smith, J. Phys. Chem. B **106**, 5194 (2002).